

Partial spectral weights of disordered $\text{Cu}_x\text{Pd}_{1-x}$ alloys including the photoemission matrix-element effect

Tschang-Uh Nahm, Moon-sup Han, and S.-J. Oh

Department of Physics, Seoul National University, Seoul 151-742, Korea

J.-H. Park and J. W. Allen

Department of Physics, University of Michigan, Ann Arbor, Michigan 48109-1120

S.-M. Chung

Department of Physics, Pohang University of Science and Technology, Pohang, 790-784, Korea

(Received 3 November 1994)

The valence-band photoemission spectra of disordered $\text{Cu}_x\text{Pd}_{1-x}$ alloys are measured with synchrotron radiation in the soft-x-ray regime. Taking advantage of the Cooper-minimum phenomenon of the Pd 4d photoionization cross section, we obtain Pd and Cu partial spectral weights of $\text{Cu}_x\text{Pd}_{1-x}$ alloys at various compositions ($x=0.1, 0.25, 0.5, 0.75, 0.9$) using the empirically determined ratio of photoionization cross sections. We find that at this photon energy the photoionization matrix element strongly suppresses structures at the high-binding-energy side of the valence-band spectra where coherent potential approximation calculations predicted appreciable bonding states between Cu 3d and Pd 4d levels. By taking the spectra at the x-ray photoemission regime where this matrix-element effect is less severe, we find that the experimental Pd partial spectral weight is in good agreement with theoretical predictions. The lattice relaxation effect does not seem very important for the suppression of Cu 3d and Pd 4d bonding states, at least for concentrated alloys studied here.

I. INTRODUCTION

The electronic structures of disordered alloys are interesting from the viewpoints of both fundamental physics and technological applications. From the material science point of view, many alloys exhibit interesting physical properties which are useful for practical applications, and the understanding of their electronic structures is the first step towards controlling these physical properties. From the physics point of view, the effects of disorder and of the lack of periodicity upon physical properties of solids are still a much unexplored area. Especially the breakdown of translational symmetry and the consequent inapplicability of Bloch's theorem pose a very difficult problem in calculating the electronic structures of alloys. Many theoretical models and approximation schemes have been proposed to overcome this difficulty, among them the most representative ones being the rigid band model, virtual crystal approximation, average t -matrix approximation, and the coherent potential approximation.¹ It is now generally agreed that the coherent potential approximation (CPA) gives the most consistent picture which agrees with many experimental data. In particular, it has been shown for $\text{Ni}_x\text{Cu}_{1-x}$ and $\text{Ag}_x\text{Pd}_{1-x}$ alloys that the photoemission spectra are in good agreement with the densities of states (DOS) calculated by the Korringa-Kohn-Rostocker coherent potential approximation (KKR CPA).^{2,3} In this respect, the electronic structure of the substitutionally disordered Cu-Pd alloy system has become the subject

of current controversy, and many experimental⁴⁻¹² and theoretical^{6,7,13-20} works have been done. An early x-ray photoemission spectroscopy (XPS) study^{4,5} concluded that the Pd impurity in noble metals, including the Cu host, forms a virtual bound state at a binding energy of less than 2 eV from the Fermi level by taking the difference spectra of diluted alloys with respect to host noble metals. However, theoretical calculations using the CPA (Refs. 6, 7, 14) or nonrelativistic KKR Green's function method¹³ predict well-resolved bonding states between Cu 3d and Pd 4d levels which lie near the bottom of the Cu 3d band in contrast to this experimental interpretation. Hence, more refined photoemission spectroscopy (PES) studies have been performed later, either applying the Clogston-Wolff model Hamiltonian to take into account the change of the host band density of states upon alloying,¹⁰ or using synchrotron radiation and the Cooper-minimum phenomenon of the Pd 4d photoionization cross section to determine the partial DOS of Cu and Pd separately.¹¹ But neither of these experimental studies found strong Cu-Pd bonding states at the bottom of the Cu 3d band which CPA calculations predicted.

Thus it was natural to doubt the validity of CPA-type calculations for predicting the DOS in Cu-Pd alloys and to seek a possible reason for this disagreement. One plausible mechanism proposed was the local lattice relaxation effect around Pd atomic sites. The metallic radius of Pd is about 7% larger than that of Cu, and so we may expect that the lattice around the Pd impurity in a Cu host is somewhat relaxed to relieve the strain, especially

in the dilute impurity limit. Indeed an extended x-ray-absorption fine structure (EXAFS) study¹² of 1% Pd impurity in a Cu host found an increase of the 0.045 ± 0.01 Å nearest-neighbor distance around the Pd site, which corresponds to about a 2% local lattice expansion. This effect will reduce the strength of the hybridization between Cu 3*d* and Pd 4*d* states, thus making weaker the bonding states between them.

The effect of the lattice relaxation on the density of states has been treated approximately within the CPA scheme with the use of a tight-binding Hamiltonian.^{16,17} This calculation as expected gives a narrower bandwidth and reduced intensity of bonding states at the bottom of the Cu 3*d* band compared with the results of the KKR-CPA method without lattice relaxation.¹⁴ The scalar relativistic KKR Green's function method also predicts such behavior assuming a 2% relaxation of the Pd atomic site.¹⁵ But even with this improvement, the agreement between theory and experiment is far from satisfactory. Furthermore, it is often difficult to disentangle various effects going into the theory which change the bandwidth and the intensity. For example, a fully relativistic KKR-CPA calculation with an improved iteration scheme,¹⁸ but which does not include the lattice relaxation effect, predicts a narrower bandwidth of the Pd partial DOS in $\text{Cu}_{75}\text{Pd}_{25}$ than a previous calculation.¹⁴ In fact, it is fair to say that a close comparison between reliable theoretical results for the Pd partial DOS in $\text{Cu}_{75}\text{Pd}_{25}$ with and without the lattice relaxation effect^{19,20} shows only a shift of 0.2–0.3 eV for bonding states and a small increase in the intensity of antibonding states, which is not enough to bring the theoretical DOS into agreement with experiment.

The purpose of this paper is to elucidate the origin of this apparent discrepancy between the Pd partial DOS obtained from photoemission experiments and that calculated from the CPA approximation in $\text{Cu}_x\text{Pd}_{1-x}$ alloys. At the same time we would like to see the evolution of Cu and Pd partial DOS as the composition x is varied, which will help to understand the important factors determining the electronic structures of alloys. For this purpose, it is important first of all to determine the experimental Cu and Pd partial DOS of $\text{Cu}_x\text{Pd}_{1-x}$ alloys in a reliable way. The methods used previously to deduce experimental partial DOS all have some drawbacks. The difference spectra method,^{4,5} which subtracts the host metal spectra from the alloy photoemission spectra, ignores the change of the host metal DOS due to impurities. The Clogston-Wolff Hamiltonian analysis¹⁰ takes this into account, but it needs parameter fitting and is only applicable for the dilute limit and therefore not suitable for the concentrated alloys studied here. The synchrotron radiation PES study using the Cooper minimum of the Pd 4*d* cross section seems most suitable for our purpose, but a previous study using this technique¹¹ unfortunately used the *atomic* cross section ratio calculated theoretically²¹ whereas the solid state effect is known to be significant for the Cooper-minimum phenomenon.²²

In this paper, we make use of the Cooper-minimum phenomenon of Pd 4*d* states to deduce the partial DOS of Cu and Pd separately, but with the use of experimen-

tally determined cross section ratios of Pd and Cu metals to include the solid state effect. We study $\text{Cu}_x\text{Pd}_{1-x}$ alloys systematically as the composition is varied from $x = 0.1$ to $x = 0.9$. In the course of this study, we came to realize the importance of the matrix-element effect for the photoemission spectra in *d*-band metals and alloys. The photoionization matrix element decreases significantly for the bonding states, reducing the spectral intensity at the high-binding-energy side compared with that near the Fermi level. It also changes depending on the incident photon energy. However, this effect has been neglected in many previous studies,¹¹ leading to inaccurate partial DOS. So in our analysis we include this matrix-element effect along with the lifetime broadening (imaginary part of the self-energy) to deduce the correct partial DOS. When these effects are properly taken into account, we find that the Pd partial DOS for $\text{Cu}_{75}\text{Pd}_{25}$ shows good agreement between theory and experiment. The lattice relaxation effect makes the agreement a little better, but it is not a major factor for the concentrated alloy case. Some of these results have been published already.²³

The organization of this paper is as follows. Following this Introduction, we describe the experimental details in Sec. II. In Sec. III, we present the photoemission spectra at different photon energies, and describe the procedure to deduce the partial DOS including the matrix-element effect by making use of the Cooper-minimum phenomenon of Pd 4*d* states. The Cu 3*d* and the Pd 4*d* partial spectral weights (PSW's) at various compositions of $\text{Cu}_x\text{Pd}_{1-x}$ alloys ($x=0.1, 0.25, 0.5, 0.75, 0.9$) thus obtained are presented in Sec. IV. Here we also compare the experimentally determined Pd PSW for $\text{Cu}_{75}\text{Pd}_{25}$ with those calculated theoretically with and without the lattice relaxation effect. In Sec. V, we discuss how the shapes of the calculated PSW's change when we include the real part of the self-energy. Also, the importance of the lattice relaxation effect for determining the DOS for alloys is discussed, as well as the possible difference between the dilute impurity limit and the concentrated alloy cases. The paper closes with a conclusion in Sec. VI.

II. EXPERIMENTAL DETAILS

Disordered $\text{Cu}_x\text{Pd}_{1-x}$ ($x = 0.1, 0.25, 0.5, 0.75, 0.9$) alloy samples were all polycrystalline made by arc melting two constituents in an atmosphere of argon gas on a water-cooled copper hearth. X-ray-diffraction measurements show the homogeneity and no presence of ordered states. The Cu-Pd alloy system has ordered phases in the range of 7–27 at. % Pd (fcc $L1_2$ structure for 7–19% and tetragonally deformed $L1_2$ -like structure for 19–27%) below 500 °C and 29–55 at. % Pd (bcc B_2 structure) below 600 °C.²⁴ To promote homogeneity and disorder, the alloy samples were annealed at 600 °C in evacuated quartz ampoules for 20 h and then quenched rapidly in cold water.

We measured the valence-band photoemission spectra of pure Cu and Pd metals and disordered $\text{Cu}_x\text{Pd}_{1-x}$ al-

loys using synchrotron radiation in the photon energy range of 40–200 eV. The spectra at this soft-x-ray regime were taken at the National Synchrotron Light Source (NSLS) Beamline U4A of Brookhaven National Laboratory, which was equipped with a 6 m/160° toroidal grating monochromator. The total resolution at the Fermi level was less than 0.3 eV full width at half maximum (FWHM) for photon energies below 160 eV. Angle-integrated photoelectron spectra were measured with a Vacuum Scientific Workshop (VSW) HA100 concentric hemispherical analyzer (CHA) with a single-channel electron multiplier. All measurements were performed under a pressure of a low 10^{-10} torr.

The valence spectra were measured also with He II lines ($h\nu = 40.8$ eV) and Mg $K\alpha$ x rays ($h\nu = 1253.6$ eV). The unpolarized He II lines from a gas discharge lamp was used for the ultraviolet PES (UPS) measurement in the VSW ESCA/Auger system at Seoul National University equipped with a HA150 CHA with a multichannel detector. The resolution was 0.22 eV FWHM at the Fermi level and the pressure was a low 10^{-8} torr during the measurement. XPS spectra were taken in the same chamber with an unmonochromatized Mg $K\alpha$ source. The resolution was 0.75 eV FWHM and the pressure was a high 10^{-10} torr.

To remove contaminations on the surface, sample surfaces were sputtered with argon ions of a kinetic energy of 1.0 keV for about 20 min and then annealed at a temperature of about 300 °C for 30 min. The spectra with He II lines were measured after scraping the sample surfaces with a diamond file. In the case of alloys, we should be careful about the compositions of the surface which may change due to a surface segregation effect from sputtering and annealing. Fortunately, it was shown for $\text{Cu}_x\text{Pd}_{1-x}$ alloys²⁵ that this effect is almost nonexistent or only leads to a very slight Pd enrichment at most, which was also confirmed from our experiments.

III. DATA AND ANALYSIS METHOD

A. Valence-band spectra in the soft-x-ray regime

Figure 1 shows the photoemission spectra of $\text{Cu}_x\text{Pd}_{1-x}$ ($x = 0.1, 0.25, 0.5, 0.75, 0.9$) alloys along with those of pure Cu and Pd metals with a photon energy of $h\nu = 40.8$ eV. At this photon energy the calculated ratio of the photoionization cross section of Pd 4d to that of Cu 3d is 3.3,²¹ and so the Pd partial DOS is emphasized. The contribution from s, p levels to the photoemission spectra can be safely neglected for both Cu and Pd in the photon energy region used in this work ($h\nu > 40$ eV).²¹ As the content of Cu increases, we can see that the intensity at the Fermi level decreases rapidly and the structure due to the Pd 4d electrons forms a shoulder at the top of the Cu 3d band.

For comparison, we also show the spectra of $\text{Cu}_{75}\text{Pd}_{25}$ and Cu at $h\nu = 60$ eV, where the calculated ratio of the photoionization cross section of Pd 4d to that of Cu 3d is 1.2.²¹ As a result, the contribution from the Cu partial DOS to the spectra is expected to be enhanced. The

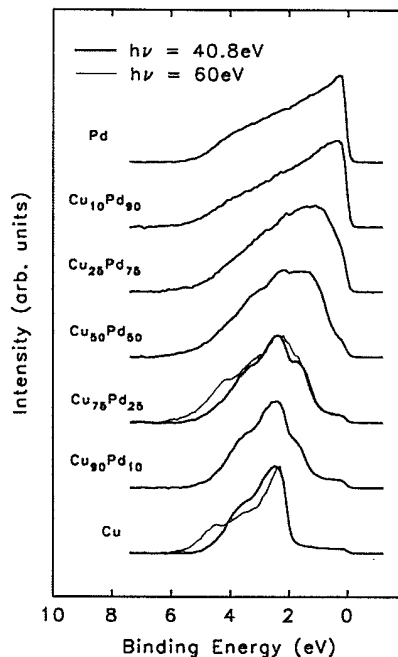


FIG. 1. Photoemission spectra of Pd, $\text{Cu}_{10}\text{Pd}_{90}$, $\text{Cu}_{25}\text{Pd}_{75}$, $\text{Cu}_{50}\text{Pd}_{50}$, $\text{Cu}_{75}\text{Pd}_{25}$, $\text{Cu}_{90}\text{Pd}_{10}$, and Cu with He II lines ($h\nu = 40.8$ eV) from the scraped surfaces. The data are drawn to have the same heights, after removing the inelastic background and correcting for the analyzer transmission function. The thin lines in the spectra of $\text{Cu}_{75}\text{Pd}_{25}$ and Cu are the spectra taken with $h\nu = 60$ eV after the sputter-anneal cleaning procedure.

spectrum of $\text{Cu}_{75}\text{Pd}_{25}$ really shows enhanced structure at $E_B = 4\text{--}6$ eV, but this enhanced structure is also seen in the Cu spectrum at $h\nu = 60$ eV. So if the $\text{Cu}_{75}\text{Pd}_{25}$ spectrum at $h\nu = 60$ eV is directly compared with the Cu spectrum at $h\nu = 40.8$ eV, the enhanced spectral weight may be incorrectly interpreted as an indication of the enhancement of the Pd partial DOS at the bonding states. This photon energy dependence of the shapes of pure metal spectra will thus be fully included in the analysis procedure of present work.

Figure 2 shows the spectra of Cu-Pd alloys along with that of pure Cu at the photon energy of 130 eV. Due to the Cooper-minimum phenomenon of Pd 4d states at this photon energy, the calculated photoionization cross section of Pd 4d is only 0.06 times that of Cu 3d,²¹ and so these spectra can be regarded as the Cu partial DOS of Cu-Pd alloys in the first approximation. As the content of Pd increases, the central position of the band shifts towards the Fermi level in accordance with the direction of the core-level shift of the Cu 2p levels,⁵ and the top of the band becomes broader due to the Cu 3d-Pd 4d hybridization.

B. Photoionization cross sections

As mentioned in the Introduction, in order to deduce the partial DOS of Cu and Pd, we will make use of the difference of alloy PES spectra due to the relative photoion-

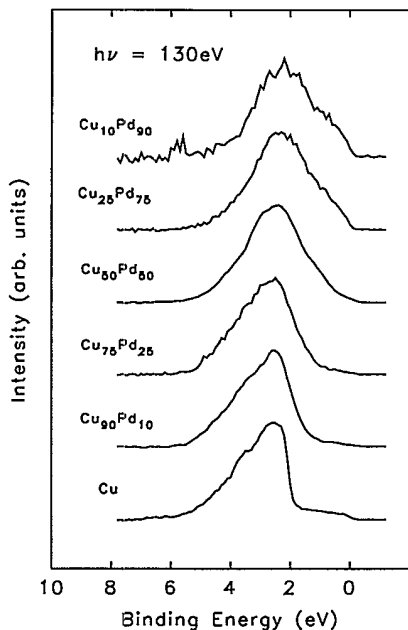


FIG. 2. Photoemission spectra of $\text{Cu}_{10}\text{Pd}_{90}$, $\text{Cu}_{25}\text{Pd}_{75}$, $\text{Cu}_{50}\text{Pd}_{50}$, $\text{Cu}_{75}\text{Pd}_{25}$, $\text{Cu}_{90}\text{Pd}_{10}$, and Cu with photon energy $h\nu = 130$ eV from the sputter-annealed surfaces. Other details are the same as in Fig. 1.

ization cross section change with photon energy. To make a quantitative analysis, it is necessary to find the cross section ratios of Pd and Cu accurately. In particular, the calculated *atomic* cross sections are not reliable, because the solid state effect is shown to be important for the Cooper-minimum phenomena,²² as one can expect from the change of these valence-band wave functions between atomic and metallic phases. In this subsection, therefore, we determine the cross section ratio as a function of photon energy by measuring the valence-band spectra of pure Cu and Pd metals. [For the moment, we will not concern ourselves with the binding energy dependence of the cross section (matrix-element effect) which will be discussed in the next subsection, but only with the total intensity variation here.]

For this purpose, we first obtain the normalized spectra of Cu and Pd metals at each photon energy using the photon flux measured by the photocurrent from a stainless steel mesh in front of the chamber. The normalized spectra are then multiplied by the kinetic energy of the photoelectron to compensate for the analyzer transmission function. The inelastic background is also removed. The change of areas of these spectra with respect to the photon energy is an indication of change in the photoionization cross section. To get the absolute change of the photoionization cross section from these areas, it is necessary to know the absorption property of the mesh. Fortunately, for our procedure of extracting partial DOS described in the next section, we only need to know the *ratios* of the photoionization cross sections between Cu and Pd *d* states. In this case, the absorption property of the mesh is canceled, and we can write

$$\frac{\sigma_{4d}^{\text{Pd}}(h\nu)}{\sigma_{3d}^{\text{Cu}}(h\nu)} = C \frac{I_{4d}^{\text{Pd}}(h\nu)}{I_{3d}^{\text{Cu}}(h\nu)}, \quad (1)$$

where $\sigma_{4d}^{\text{Pd}}(h\nu)$ [$\sigma_{3d}^{\text{Cu}}(h\nu)$] is the cross section of the Pd 4*d* [Cu 3*d*] state at the photon energy $h\nu$, $I_{4d}^{\text{Pd}}(h\nu)$ [$I_{3d}^{\text{Cu}}(h\nu)$] is the area of the normalized PES spectrum of Pd [Cu] metal at that photon energy, and C is the proportionality constant.

The proportionality constant C is determined in the following way. Since the photoyield depends sensitively on extrinsic factors such as the smoothness of the sample surface, the angle between the sample surface and the analyzer and so on in addition to the photoionization cross section, it is necessary to find a normalization constant which is independent of these extrinsic factors. Here we choose the intensities of the Pd 4*p* and the Cu 3*p* core-level emissions in the XPS spectra of pure metals as the normalization constants. Because the binding energies of these two core levels are very close, the inelastic mean free path of photoelectrons at the XPS regime should be nearly the same. And since we expect that the wave functions of core electrons in solids do not change very much between atomic and solid phases, we can use the calculated atomic cross sections of these core levels²¹ on the left hand side of the equation

$$\frac{\sigma_{4p}^{\text{Pd}}(\text{Mg } K\alpha)}{\sigma_{3p}^{\text{Cu}}(\text{Mg } K\alpha)} = C \frac{I_{4p}^{\text{Pd}}(\text{Mg } K\alpha)}{I_{3p}^{\text{Cu}}(\text{Mg } K\alpha)}$$

to determine the proportionality constant C by measuring the areas of core level photoemission spectra on the right hand side of this equation.

The resulting cross section ratios are shown in Fig. 3 along with the result of atomic cross section calculations.²¹ The differences between theoretical and experimental results are the shift of the dip position of the Cooper minimum of Pd 4*d* around $h\nu = 130$ eV, which is in agreement with a previous report,²² and the decrease of the ratio of the photoionization cross section

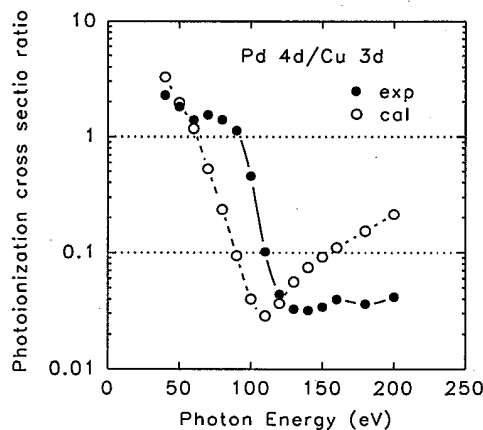


FIG. 3. Ratios of the photoionization cross section of Pd 4*d* to that of Au 5*d* at a photon energy between 40 eV and 200 eV. Solid circles are experimental points from pure metals, and open circles are calculated atomic values (Ref. 21). Note the small values at photon energies around 130 eV due to the Cooper minimum of Pd 4*d* states.

of Pd 4d to that of Cu 3d at higher photon energies than 130 eV when experimentally determined. These are due to the solid state effect which deforms the wave functions of the valence bands. The ratios at about 50 eV agree with each other, but at 130 eV, the empirically determined value is about half that of the atomic calculation. The empirical value at $h\nu = 40.8$ eV determined from Eq. (1) is 2.2 which is smaller than the result of the atomic calculation, 3.3.²¹

C. Procedure to extract partial spectral weights

In this subsection, we develop a procedure for extracting partial spectral weights of alloys by using the change of the photoionization cross section with incident photon energy. We take the matrix element effect into account to include the change in the shapes of the pure metal spectra as the photon energy is varied. For the photon energy $h\nu$ sufficiently high (XPS regime), the angle-integrated photocurrent $I(E, h\nu)$ from multicomponent solids with an electron binding energy E can be expressed as²⁶

$$I(E, h\nu) \propto \sum_{\alpha, j} x_{\alpha} \sigma_j^{\alpha}(E, h\nu) \rho_j^{\alpha}(E). \quad (2)$$

Here x_{α} is the concentration of the constituent atom α , $\sigma_j^{\alpha}(E, h\nu)$ is total angular-momentum-dependent photoionization matrix element of the constituent α , generally referred to as the photoionization cross section in the atomic view, j is the angular momentum, and $\rho_j^{\alpha}(E)$ is the partial DOS of the constituent atom α with angular momentum j . Here and henceforth, we will assume that the photoemission spectral intensity $I(E, h\nu)$ is normalized to the photon flux, and the analyzer transmission function ($1/E$ correction is applied in this work) as well as the inelastic background corrections have been performed. Equation (2) becomes inapplicable when the incident photon energy is so low that the assumption of the quasicontinuum final state fails due to the small number of final states available in k space;²⁶ hence the assumption of no interference of final states from different atomic sites fails.¹⁴ This assumption, generally known as the local approximation, can be regarded to hold for a photon energy as low as 40 eV,²⁶ and therefore Eq. (2) can be safely used throughout this paper.

For the Cu-Pd alloy problems at hand, we can simplify Eq. (2) somewhat. Since the photoionization cross sections of s or p electrons are very small compared with d cross sections at this photon energy range for both Cu and Pd atoms,²¹ we can neglect s, p contributions to the photoemission spectra. Furthermore, the spin-orbit couplings of 3d and 4d elements are not large compared to those of 5d elements. Hence we can drop the summation over j and write

$$I(E, h\nu) \propto \sum_{\alpha} x_{\alpha} \sigma^{\alpha}(E, h\nu) \rho^{\alpha}(E), \quad (3)$$

where $\rho^{\alpha}(E)$ is the partial DOS of the d band of the constituent α , and $\sigma^{\alpha}(E, h\nu)$ is the matrix element. What we want to extract here is the partial DOS $\rho^{\alpha}(E)$, and so

it is necessary to determine $\sigma^{\alpha}(E, h\nu)$, or at least the ratio between them. However, as emphasized in our earlier publication,²³ the matrix element in the photoionization process $\sigma^{\text{Cu}}(E, h\nu)$ has a strong binding energy dependence in d bands due to the solid state effect in addition to the photon energy dependence.²⁷ Because of this fact, a simple subtraction of spectra at different photon energies does not work. Hence we develop an approximate, but more accurate, procedure of extracting the PSW's of binary alloys, taking into consideration the matrix-element effect in the photoemission process in the following way.

We first rewrite Eq. (3) as

$$I(E, h\nu) \propto \sum_{\alpha} x_{\alpha} \bar{\sigma}^{\alpha}(h\nu) n^{\alpha}(E, h\nu) \quad (4)$$

by defining the PSW of the α constituent $n^{\alpha}(E, h\nu)$ with the relation

$$n^{\alpha}(E, h\nu) = \sigma_0^{\alpha}(E, h\nu) \rho^{\alpha}(E), \\ \int dE n^{\alpha}(E, h\nu) = \int dE \rho^{\alpha}(E). \quad (5)$$

In effect, the binding energy dependence of the matrix element is included in the partial spectral weight $n^{\alpha}(E, h\nu)$ by means of $\sigma_0^{\alpha}(E, h\nu)$, and $\bar{\sigma}^{\alpha}(h\nu)$ in Eq. (4) is a binding-energy-independent value representing the total intensity change with photon energy which we have determined in the previous subsection. Note that in the presence of the matrix-element effect the PSW is the quantity actually measured experimentally rather than the DOS. Now we will make the assumption that $\sigma_0^{\alpha}(E, h\nu)$ and $\bar{\sigma}^{\alpha}(h\nu)$ do not change between pure metals and alloys. Then using the value of $\bar{\sigma}^{\alpha}(h\nu)$ which was determined in the previous subsection for pure metals, we can determine $n^{\alpha}(E, h\nu)$ by measuring $I(E, h\nu)$ of alloys at two different photon energies (in our case $h\nu = 40.8$ eV and $h\nu = 130$ eV were used) in the following way.

As can be seen in Fig. 3, the ratio of $\sigma_{4d}^{\text{Pd}}(h\nu)$ to $\sigma_{3d}^{\text{Cu}}(h\nu)$ [these σ 's are in fact $\bar{\sigma}$'s in the notation of Eq. (4)] is 2.2 and 0.03 at $h\nu = 40.8$ eV and 130 eV, respectively. Taking full advantage of this Cooper-minimum phenomenon, we can assume as a first step that the spectra of alloys at $h\nu = 130$ eV are nearly the same as the Cu PSW of alloys at $h\nu = 130$ eV, i.e.,

$$n_{\text{alloy}}^{\text{Cu}}(E, 130 \text{ eV}) \simeq I_{\text{alloy}}(E, 130 \text{ eV}), \quad (6)$$

where the subscript stands for the sample and the superscript for the constituent atom. From Eq. (5) two spectra of Cu metal at $h\nu = 40.8$ eV and at $h\nu = 130$ eV can be related to the matrix elements of the Cu 3d states at those photon energies as follows:

$$\frac{\sigma_0^{\text{Cu}}(E, 40.8 \text{ eV})}{\sigma_0^{\text{Cu}}(E, 130 \text{ eV})} = \frac{I_{\text{Cu}}^{\text{norm}}(E, 40.8 \text{ eV})}{I_{\text{Cu}}^{\text{norm}}(E, 130 \text{ eV})},$$

where $I_{\text{Cu}}^{\text{norm}}(E, 40.8 \text{ eV})$ and $I_{\text{Cu}}^{\text{norm}}(E, 130 \text{ eV})$ are pure Cu metal spectra at two photon energies which are normalized to have the same area. The divided spectrum obtained in this way can be used for any composition of Cu-Pd alloys under our assumption that the matrix ele-

ment does not change from metals to alloys, and therefore we can write

$$n_{\text{alloy}}^{\text{Cu}}(E, 40.8 \text{ eV}) \simeq \frac{\sigma_0^{\text{Cu}}(E, 40.8 \text{ eV})}{\sigma_0^{\text{Cu}}(E, 130 \text{ eV})} n_{\text{alloy}}^{\text{Cu}}(E, 130 \text{ eV}), \quad (7)$$

$$n_{\text{alloy}}^{\text{Pd}}(E, 40.8 \text{ eV}) \simeq I_{\text{alloy}}^{\text{norm}}(E, 40.8 \text{ eV}) \left[1 + \frac{x^{\text{Cu}} \bar{\sigma}_{3d}^{\text{Cu}}(40.8 \text{ eV})}{x^{\text{Pd}} \bar{\sigma}_{4d}^{\text{Pd}}(40.8 \text{ eV})} \right] - n_{\text{alloy}}^{\text{Cu}}(E, 40.8 \text{ eV}) \frac{x^{\text{Cu}} \bar{\sigma}_{3d}^{\text{Cu}}(40.8 \text{ eV})}{x^{\text{Pd}} \bar{\sigma}_{4d}^{\text{Pd}}(40.8 \text{ eV})}, \quad (8)$$

where $I_{\text{alloy}}^{\text{norm}}(E, 40.8 \text{ eV})$ is the alloy spectra at $h\nu = 40.8 \text{ eV}$ which is normalized to have the same area as $n_{\text{alloy}}^{\text{Cu}}(E, 40.8 \text{ eV})$.

The resulting PSW's are not yet self-consistent since $n_{\text{alloy}}^{\text{Pd}}(E, 40.8 \text{ eV})$ is obtained using $n_{\text{alloy}}^{\text{Cu}}(E, 130 \text{ eV})$ of Eq. (6), which assumes that the contribution from Pd states, $n_{\text{alloy}}^{\text{Pd}}(E, 130 \text{ eV})$, to the alloy spectra at $h\nu=130 \text{ eV}$ [$I_{\text{alloy}}(E, 130 \text{ eV})$] is zero. We use iterations to correct for this inconsistency. The procedure is the same as above, but now we use $n_{\text{alloy}}^{\text{Pd}}(E, 40.8 \text{ eV})$ obtained in Eq. (8) and the cross section ratios determined in Fig. 3 to obtain a more correct representation of the Cu PSW of alloys at $h\nu = 130 \text{ eV}$, after correcting for the matrix-element effect of Pd metal between $h\nu = 40.8 \text{ eV}$ and $h\nu = 130 \text{ eV}$. With this new Cu PSW at $h\nu = 130 \text{ eV}$, we repeat the process in Eqs. (7) and (8) to obtain a better result of the Pd PSW at $h\nu = 40.8 \text{ eV}$. Iterations of 4 or 5 times are enough to obtain the convergence to self-consistent results.

This procedure is similar to that used in Ref. 11 to analyze the spectra of $\text{Cu}_{75}\text{Pd}_{25}$, and when we apply our procedure to the spectra of $\text{Cu}_{75}\text{Pd}_{25}$, we find that the overall structures of the resulting PSW's are similar. But the neglect of the matrix-element effect and the use of the calculated values of the atomic photoionization cross sections in Ref. 11 lead to somewhat inaccurate PSW's. For example, the Pd PSW deduced there depends on the photon energy used. Especially when the spectra at $h\nu = 50$ or 60 eV is used to extract the Pd PSW by subtracting the spectra at $h\nu = 130 \text{ eV}$, they find substantial intensity at the binding energy $E_B \simeq 5 \text{ eV}$. This is because the spectra of Cu and $\text{Cu}_{75}\text{Pd}_{25}$ at $h\nu = 60 \text{ eV}$ have an appreciable amount of spectral weight at $E_B \simeq 5 \text{ eV}$ relative to that at $h\nu = 130 \text{ eV}$, as can be seen in Figs. 1 and 2.

IV. PARTIAL SPECTRAL WEIGHTS OF $\text{Cu}_x\text{Pd}_{1-x}$ ALLOYS

A. Cu and Pd PSW's in the soft-x-ray regime

Figure 4 shows the Cu PSW's at various compositions of $\text{Cu}_x\text{Pd}_{1-x}$ alloys ($x=0.1, 0.25, 0.5, 0.75, 0.9$) determined from our procedure described above. As anticipated, the Cu PSW's are quite similar to the spectra at $h\nu = 130 \text{ eV}$ because of the strong Cooper-minimum phenomenon of Pd 4d states. Nearly no change is observed for the bonding states, but this is at least in part

which is the approximate Cu PSW of the Cu-Pd alloy at $h\nu = 40.8 \text{ eV}$. This in effect corrects for the change of the shape in the Cu spectra from $h\nu = 130 \text{ eV}$ to $h\nu = 40.8 \text{ eV}$. Now that the ratio of $\bar{\sigma}_{4d}^{\text{Pd}}(40.8 \text{ eV})$ to $\bar{\sigma}_{3d}^{\text{Cu}}(40.8 \text{ eV})$ is 2.2, it is possible to obtain the Pd PSW at $h\nu = 40.8 \text{ eV}$ using Eq. (4),

due to the matrix-element effect of Cu 3d states at $h\nu = 130 \text{ eV}$ which suppresses the intensity of bonding states. The central position of the Cu PSW moves a little toward the Fermi level as the Cu content decreases.

For $\text{Cu}_{10}\text{Pd}_{90}$, the central position of the Cu PSW is at $E_B \simeq 2.5 \text{ eV}$, well inside the Pd 4d band. Moreover, the Cu 3d-Pd 4d hopping matrix-element in a Pd host is 1.2 times that of Cu 3d-Cu 3d in pure Cu metal according to the Harrison's tight-binding scheme.²⁸ Hence it is expected that the bandwidth of the Cu partial DOS is not small even for Cu-diluted alloys. Indeed, the Cu PSW shown in Fig. 4 confirms that the bandwidth is nearly the same, if not larger, as that of pure Cu. This fact has already been observed with the Cu $L_{2,3}\text{-}M_{4,5}$ x-ray spectra of $\text{Cu}_{10}\text{Pd}_{90}$,⁸ and it means that the band of $\text{Cu}_{10}\text{Pd}_{90}$ is a common-band type and does not show split-band behavior.

Figure 5 shows the Pd PSW's of Cu-Pd alloys at various compositions. As the Pd content decreases, the number of DOS at the Fermi level decreases rapidly, and peaks at $E_B = 1.8 \text{ eV}$ become prominent. Comparing the

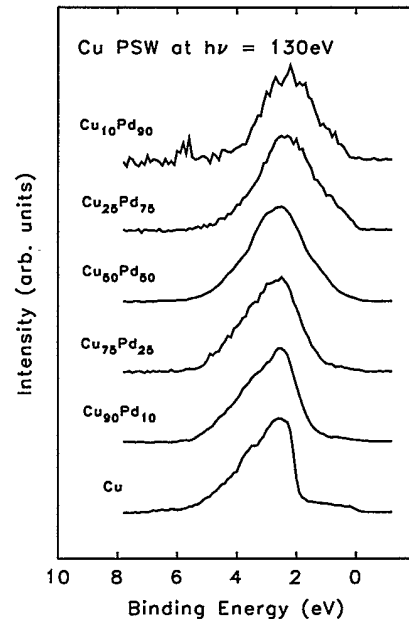


FIG. 4. Empirical Cu partial spectral weights of Cu-Pd alloys at $h\nu = 130 \text{ eV}$ using the experimentally determined photoionization cross section ratio and including the matrix-element effect.

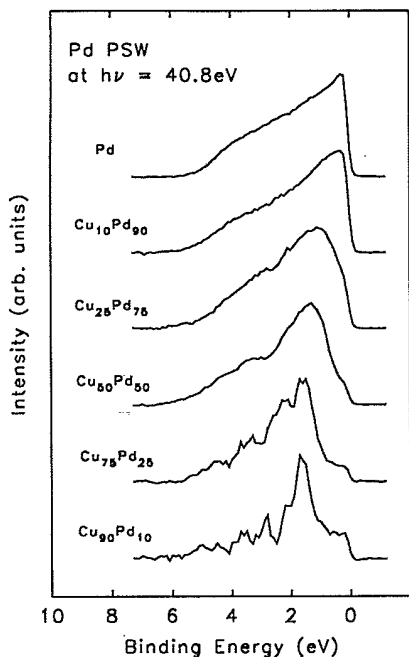


FIG. 5. Empirical Pd partial spectral weights of Cu-Pd alloys at $h\nu = 40.8$ eV using the experimentally determined photoionization cross section ratio and including the matrix-element effect. The intensity of the bonding state is very small due to the matrix-element effect of Pd $4d$ states.

Pd PSW's of Pd-diluted alloys with the spectra of pure Pd metal, it seems that the intensity of bonding states for alloys at the higher-binding-energy side is somewhat reduced, especially for the $\text{Cu}_{90}\text{Pd}_{10}$ case. But it is difficult to say quantitatively because of the strong matrix-element effect at $h\nu = 40.8$ eV which suppresses the photoemission intensity of bonding states. This trend is at least consistent with what we expect from the Harrison's tight-binding scheme.²⁸ In Pd-diluted Cu-Pd alloys, the Pd $4d$ -Cu $3d$ hopping matrix-element is 0.75 times that of Pd $4d$ -Pd d in pure Pd metal. The difference between the central positions of the Cu $3d$ band and Pd $4d$ band is larger than 1 eV, and this will also reduce the mixing of Pd $4d$ states with Cu $3d$ states compared to the hybridization between Pd $4d$ states in pure Pd. Hence the bonding states are expected to be weaker.

B. Pd PSW of $\text{Cu}_{75}\text{Pd}_{25}$ and comparison with theory

In this section, we try to answer the question of the validity of the CPA calculation for Cu-Pd alloys and of the importance of the lattice relaxation effect in determining the DOS of alloys. For this purpose, we compare the Pd PSW of $\text{Cu}_{75}\text{Pd}_{25}$ quantitatively between theory and experiment, since the $\text{Cu}_{75}\text{Pd}_{25}$ alloy has been studied before both experimentally and theoretically^{11,14,19} in this respect. But previous studies did not take into account the photoionization matrix-element effect in the experimental Pd PSW. As seen above, the matrix-element effect suppresses the high-binding-energy structure in the

Pd PSW when photons at the soft-x-ray regime are used, and so it is difficult to compare theoretical DOS with experimental spectra quantitatively. It would be much better if we could measure the PES spectra at a photon energy where the variation of the matrix element within the band is not so pronounced. As can be seen in Fig. 6(a), the XPS spectra are better in this respect since they show more weight in the higher-binding-energy region than the UPS spectra for both Cu and Pd. Even in this case, however, we can see from comparing with the theoretical DOS (Ref. 29) in Fig. 6(b) that the XPS spectrum of Pd still has less weight and structure in the high-binding-energy region. The origin of this discrepancy is again the photoionization matrix-element effect, although not as pronounced as in the UPS regime, and the lifetime broadening.

To see whether these factors can be taken into account quantitatively for a meaningful comparison between theory and experiment, we try to fit the experimental XPS spectra with the theoretical DOS for pure Pd metal by considering these effects. For this purpose, we first multiply the theoretical Pd $4d$ DOS of Pd metal with the calculated matrix element in the XPS region,²⁷ and then include lifetime broadening assuming the Fermi liquid behavior. The resulting curve is convoluted with the Gaussian function for the instrumental broadening. By this method, we could get very good agreement between experimental and theoretical spectra

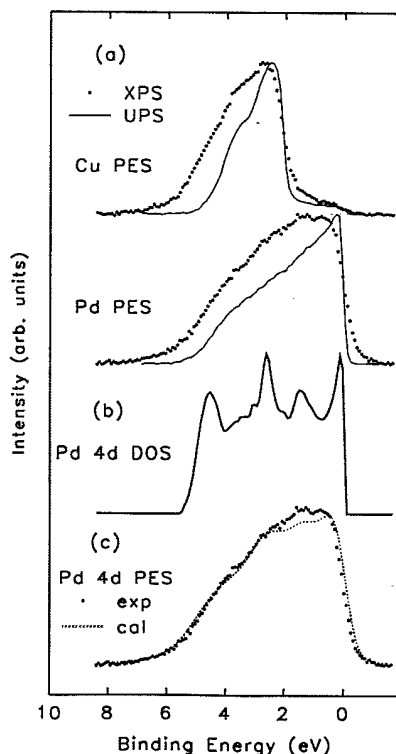


FIG. 6. (a) UPS and XPS spectra of pure Cu and Pd metals. (b) Calculated Pd $4d$ DOS of pure Pd metal (Ref. 29). (c) The fit of the Pd metal XPS spectrum after including the matrix-element effect with lifetime and instrumental broadening effects.

for Pd metal as shown in Fig. 6(c). Here we choose the lifetime broadening parameter with the Lorentzian form whose half-width increases quadratically from zero at the Fermi level to 1.5 eV at $E_B = 8.4$ eV (this corresponds to the broadening of 0.67 eV at the bottom of the Pd 4d band, $E_B = 5.6$ eV), and the instrumental broadening is represented by a Gaussian function of 0.75 eV FWHM, which reproduces the experimental spectra at the Fermi level. The Lorentzian width of 0.67 eV at the bottom of the band may seem somewhat large, but a similar value has been used before to bring the experimental XPS spectra of the pure Pt valence band into agreement with the result of KKR band calculations.³⁰ There has been some concern³¹ that this lifetime broadening represented by the imaginary part of the self-energy [$\text{Im } \Sigma(E)$] may induce appreciable shifts of spectral weights due to $\text{Re } \Sigma(E)$, since these two quantities are related by the Kramers-Kronig relation. We will return to this point in Sec. V.

Since it seems possible to include the lifetime broadening and matrix-element effects quantitatively in the XPS spectra, we now obtain the Pd PSW of $\text{Cu}_{75}\text{Pd}_{25}$ in the XPS ($h\nu = 1253.6$ eV) regime, $n_{\text{alloy}}^{\text{Pd}}(E, 1253.6 \text{ eV})$, by the same procedure as before using the spectra at $h\nu = 1253.6$ eV and at $h\nu = 130$ eV. Again we assume that the matrix-element is the same for pure metals and alloys, which is justified by a theoretical calculation³⁰ showing that the matrix element at a photon energy of the XPS regime changes only marginally with respect to the concentration including pure metals. During this procedure the spectra at $h\nu = 130$ eV were broadened to account for the difference of the instrumental resolution with XPS spectra, and the ratio between the photoionization cross section of Pd 4d states to that of Cu 3d was experimentally determined to be 1.67, which is a little larger than the calculated atomic value of 1.24 for the Mg $K\alpha$ source.²¹ Thus the obtained Pd PSW $n_{\text{alloy}}^{\text{Pd}}(E, 1253.6 \text{ eV})$ is shown in Fig. 7(a) by dots. Compared to the empirical PSW determined at $h\nu = 40.8$ eV shown in the same figure with a line, it shows a noticeable increase in the intensity of bonding states in the XPS regime due to the difference of the matrix-element effect. The peak position of the antibonding states does not change, and there is a structure at $E_B = 3\text{--}4$ eV and a broad tail extends to $E_B \sim 7$ eV.

To see how this experimental Pd PSW compares with the theoretical calculations and to assess the importance of the lattice relaxation effect in alloy DOS, we show in Fig. 7(b) the calculated Pd partial DOS of $\text{Cu}_{75}\text{Pd}_{25}$ from the self-consistent relativistic KKR-CPA method without a lattice relaxation effect (thick line),¹⁸ and that of the special quasirandom structure (SQS) band calculation which takes into account the local lattice relaxation effect (thin line).¹⁹ The SQS calculation makes use of a superlattice structure having a distribution of distinct environments such that their average corresponds to a real random medium while the atomic sites are fully relaxed.¹⁹ The lattice spacings in this superlattice are determined to have the minimum energy in a given volume. The comparison of these two calculations in Fig. 7(b) shows that the SQS calculation indeed gives a smaller weight of

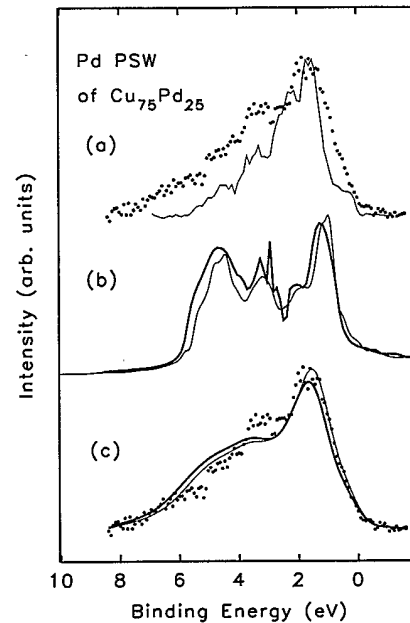


FIG. 7. (a) Pd partial spectral weight of $\text{Cu}_{75}\text{Pd}_{25}$ at $h\nu = 40.8$ (line) and 1253.6 eV (dots). (b) Calculated Pd partial DOS of $\text{Cu}_{75}\text{Pd}_{25}$ using the KKR CPA without the lattice relaxation effect (Ref. 18, thick line) and using SQS which effectively includes lattice relaxation assuming a superlattice structure (Ref. 19, thin line). The SQS result is smoothed using a Gaussian function with a half width at half maximum (HWHM) = 0.2 eV. (c) Comparison of the experimental XPS Pd PSW (dots) with the calculated spectral weights using band calculation of Refs. 18 (thick line) and 19 (thin line) after including the matrix-element effect and lifetime as well as instrumental broadening effects.

bonding states than in the unrelaxed KKR-CPA calculation, which will bring the theoretical DOS closer to the experimental PSW. But the magnitude of this difference is not big enough to supply agreement with experiment. Also the shift of the binding energy of bonding states is not very large, when the shift of antibonding states of the relaxed structure toward the Fermi level is taken into consideration.

To compare these theoretical Pd DOS and the experimental Pd PSW quantitatively, we must include the matrix element, lifetime broadening, and instrumental broadening effects. Figure 7(c) shows this comparison between the experimental Pd PSW in the XPS regime (dots), the calculated PSW from the KKR-CPA calculation without lattice relaxation (thick line), and that from the SQS calculation with lattice relaxation (thin line). We can note two things from this figure. First, the lattice relaxation effect is not very big for the Pd DOS, far less than the discrepancy between theory and experiment. Second, the prominent peak at $E_B = 4.5$ eV of the theoretical DOS is completely smeared out and reduced in intensity partly due to the lifetime broadening and partly due to the matrix-element effect, bringing the theoretical spectra into reasonable agreement with the experimentally determined PSW. This resolves much of the discrepancy between theory and experiment in previ-

ous studies which did not consider the important matrix-element effect. It is fair to say that even if the Pd partial DOS had strong structures at $E_B \simeq 4.5$ eV, it could not be clearly resolved with XPS, and almost impossible to see with UPS.

It should be mentioned that in the comparison of Fig. 7(c) both theoretical DOS are shifted downward by 0.65 eV to make the antibonding peak near the Fermi level align with experimental spectra. This amount of shift is also found to be necessary to match the experimentally determined Cu PSW of $\text{Cu}_{75}\text{Pd}_{25}$ in Fig. 4 with the theoretical calculations. The reason for this shift is the inaccurate Fermi level position predicted in theoretical calculations for noble metals and alloys, which is well known and seen in many studies.^{32,33}

V. DISCUSSION

A. Inclusion of $\text{Re } \Sigma$

In the previous section when we fit the XPS spectrum of the Pd metal and alloy, we simply broadened the theoretical DOS by a Lorentzian function to simulate the lifetime broadening. This means that we used phenomenological values of the imaginary part of the self-energy ($\text{Im } \Sigma$), but neglected its real part ($\text{Re } \Sigma$). Some argued that this is not justified because the shifts produced by $\text{Re } \Sigma$ will likely be important.³¹ The real and imaginary parts of the self-energy are related by the Kramers-Kronig relation,³⁴ and in principle both should be included when calculating theoretical spectral weights. So we checked for this possibility by constructing a realistic form of the self-energy as follows.

To our knowledge, there is no first principles calculation of the $\Sigma(E)$ of the Pd $4d$ states.³⁵ So we borrowed the self-energy form calculated for Ni metal using the

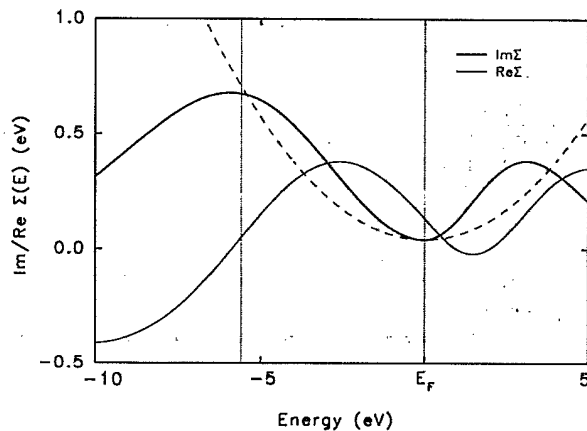


FIG. 8. Self-energy form used in calculating Pd $4d$ spectral weights. Thick (thin) line is the imaginary (real) part of the self-energy. Dashed curve is the phenomenological lifetime broadening used in Sec. IV, which increases quadratically with the binding energy from the Fermi level (Fermi liquid behavior). Vertical dotted line represents the bottom of $4d$ band of pure Pd metal.

degenerate Hubbard model,³⁶ and constructed a simplified form of $\Sigma(E)$ which has the value of $\text{Im } \Sigma$ similar to that used in the previous section. This is shown in Fig. 8, where its real and imaginary parts are related by the Kramers-Kronig relation. In this figure the phenomenological (Fermi liquid type) lifetime broadening of the previous section is also shown by the dashed line, and the dotted vertical line designates the theoretical bottom of the d band in Pd metal. We can see that the real part of the self-energy is small within the occupied valence band, which is consistent with the conclusion of an angle-resolved photoemission study.³⁷

Figure 9 shows the result of spectral weight calculations for Pd metal and Pd PSW of $\text{Cu}_{75}\text{Pd}_{25}$ using this self-energy form, and the comparison with the experimental spectrum. We see that the changes brought by the inclusion of $\text{Re } \Sigma$ are minimal, and the overall structures remain the same as before. Thus we can conclude that the neglect of $\text{Re } \Sigma$ in the previous section does not lead to a severe error in comparing the calculated and experimentally determined PSW's.

B. Auger line-shape analysis in dilute alloys

The reduction of the bonding states in Pd-diluted Cu-Pd alloys due to the lattice relaxation effect was also argued by the detailed Pd $M_{4,5}N_{4,5}N_{4,5}$ Auger line shape analysis.¹² It was shown in Pd-diluted Ag-Pd alloys^{38,39} that this Pd CVV Auger line shape is very sensitive to the Pd one-hole density of states in the region of $U + \epsilon_d^{\text{imp}}$ where U is the Pd d - d Coulomb interaction en-

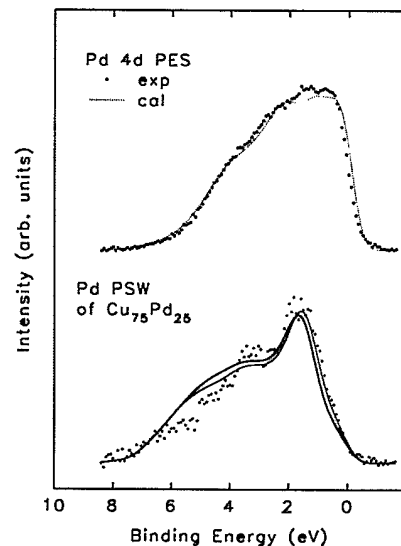


FIG. 9. Spectral weights calculated using the model self-energy of Fig. 8. Top panel shows the XPS spectra (dots) and the calculated spectral weight (solid line) of Pd metal. Bottom panel shows the comparison of the XPS Pd PSW (dots) of $\text{Cu}_{75}\text{Pd}_{25}$ with the calculated spectral weights using band calculations of Refs. 18 (thick line) and 19 (thin line). Both calculated results include the matrix-element effect and instrumental broadening.

ergy. Hence, in the case of Cu-Pd alloys, the Pd *MNN* Auger line shape is expected to be very sensitive to the Pd bonding density of states. Indeed it was reported in the case of $\text{Cu}_{95}\text{Pd}_{05}$ that the Pd *MNN* Auger profile can only be fitted with a much lower Pd bonding DOS than predicted by the KKR-CPA calculation.^{9,12} This was taken as the evidence for the importance of the lattice relaxation effect in the electronic structure of Cu-Pd alloys.¹²

There are a few shortcomings in this argument, however. First, the effect of lattice relaxation on the hopping matrix element between Cu and Pd *d* states had to be assumed to be at least twice as large as predicted by Harrison's scheme²⁸ when they tried to fit the experimental Auger profile of $\text{Cu}_{95}\text{Pd}_{05}$ in Ref. 12. Second, the formalism used for the Auger profile analysis did not include the two-hole Auger matrix-element effect, i.e., its dependence on the binding energy. This effect arises from the difference of overlap integrals in the Auger matrix-element when final state orbitals participate in bonding, and was shown to be important for the case of the $V L_3VV$ Auger spectra of V-C,⁴⁰ and also in the quantitative analysis of Si $L_{2,3}VV$ Auger spectra.⁴¹ In fact, this binding energy dependence of the Auger matrix-element effect was once proposed to be the cause of the discrepancy between theoretical and experimental Pd *MNN* Auger profiles in $\text{Cu}_{95}\text{Pd}_{05}$.⁹ Third, the lattice relaxation effect in Pd-diluted Ag-Pd alloys was not taken into account. A systematic study of the lattice distortion of solute atoms in metals by x-ray-absorption fine structure⁴² found that the Pd atomic site in the Pd-diluted Ag-Pd alloy is contracted to have a 0.9% smaller nearest neighbor distance than that of pure Ag. This is in contrast to the Pd-diluted Cu-Pd alloy case where the Pd atomic site is found to be expanded by 1.5%. So the stronger hybridization between the impurity Pd *4d* state and host Ag *4d* band in Ag-Pd alloys is anticipated as a result. But the quasiautomatic fittings of Pd *MNN* Auger spectra in $\text{Ag}_{30}\text{Pd}_{20}$ and $\text{Cu}_{95}\text{Pd}_{05}$ show that in both cases better agreement between theory and experiment is obtained when the Pd partial DOS is reduced than those calculated by the KKR CPA.⁹

All of these facts point to the importance of the two-hole Auger matrix-element effect in the quantitative fitting of Auger profiles, which plays a role at least as important as the lattice relaxation effect. In this connection, we note that Vos *et al.* fitted the Pd impurity Auger spectra in the Ag host very successfully with the calculated impurity DOS without considering the lattice contraction effect.³⁸ This may have resulted from the cancellation of two effects, the lattice relaxation (contraction) which increases the number of bonding states and the binding energy dependence of the Auger matrix element which will reduce the contribution from the bonding states.⁴³

We agree that the lattice relaxation effects in disordered binary alloy systems are important in the precise determination of electronic structures of these materials. But the issue here is a quantitative one, whether the lattice relaxation effect can explain the discrepancy between theoretical DOS and experimental photoemission spec-

tra. Calculations^{19,20} show that the lattice relaxation effect generally reduces the bandwidth of the material by less than 0.3 eV in the concentrated alloys, and the ratio of spectral weights between bonding states and antibonding states does not change much. Figures 7(b) and 7(c) clearly show that the change produced by the lattice relaxation is not enough to bring the theoretical DOS into agreement with the experimental spectral weight, but that the photoemission one-hole matrix element is more responsible for this discrepancy for the $\text{Cu}_{75}\text{Pd}_{25}$. The lattice relaxation effect in the dilute impurity limit will be clearly larger than in the concentrated alloy case, but the Pd *MNN* Auger analysis mentioned above suggests that even in this limit the matrix-element effect is at least as important as the lattice relaxation effect. We should remember in this connection that the relaxation of the Pd atomic site in the Pd-diluted Cu-Pd alloy is not a special case. Most disordered alloys experience a local distortion near the impurity, and the Pd-diluted Cu-Pd alloy is nothing but a moderate case.⁴²

VI. CONCLUSION

In this work, we investigated the electronic structure of disordered Cu-Pd alloys using synchrotron radiation PES, UPS, and XPS. With the empirically determined ratio of the photoionization cross section between Cu *3d* and Pd *4d* states, we obtained Cu *3d* and Pd *4d* PSW's of alloys as a function of composition. We used the spectra at $h\nu = 40.8$ eV where the Pd cross section is stronger and those at $h\nu = 130$ eV where the Cooper minimum of Pd *4d* occurs. The major assumption used in this procedure was that the matrix-element effects in alloys are the same as those in pure metals. The Pd PSW's determined at the soft-x-ray regime seemed far from in accordance with the KKR-CPA calculations as in other work.¹² But we showed that the main reason for this discrepancy is not the failure of the KKR-CPA scheme which cannot include the lattice relaxation effect but the result of the strong matrix-element effect which obscures the accurate determination of the Pd partial DOS in the high-binding-energy (bonding state) region.

Hence we performed XPS of $\text{Cu}_{75}\text{Pd}_{25}$, where the matrix-element effect is less severe for suppressing bonding states. The empirically determined Pd PSW of $\text{Cu}_{75}\text{Pd}_{25}$ at $h\nu = 1253.6$ eV showed two structures, one the sharp peak near the Fermi level and the other a plateau with a broad tail. Taking the matrix-element effect into consideration properly, we compared the empirically determined Pd PSW with the theoretical PSW's calculated from the revised version of KKR-CPA scheme¹⁸ and from the SQS band calculation.¹⁹ In contrast to previous comparisons without the matrix-element effects,¹¹ we found reasonably good agreement overall after correcting for the error of the Fermi level position in the theoretical calculations.

From this work, it becomes clear that a correct analysis procedure must be used to obtain the angle-integrated PSW of binary alloys and to compare with the theoretical partial DOS. The procedure must include both

the lifetime broadening and the (one-hole) photoemission matrix-element effect which can strongly deform the spectra especially for *d*-band metals and alloys. Similarly, the two-hole Auger matrix-element effect has to be considered in the quantitative analysis of the *CVV* Auger spectra.

ACKNOWLEDGMENTS

We thank Professor G. A. Sawatzky and Dr. P. J. Durham, Dr. A. Zunger, and Dr. Z. W. Lu for interesting

correspondence. We also thank Dr. G. K. Wertheim of AT&T Bell Laboratories for letting us use his equipment at NSLS. This work was supported in part by a grant from the Korean Ministry of Education. The soft-x-ray photoemission was carried out at NSLS, Brookhaven National Laboratory, which is supported by the U.S. Department of Energy (DOE), Division of Materials Sciences and Division of Chemical Sciences. Work at the University of Michigan was also supported by the U.S. DOE Contract No. DE-FG02-90ER45416. Travel funds to NSLS were provided by the user program of the Pohang Light Source, Korea.

- ¹ For a review, see, for example, H. Ehrenreich and L.M. Schwartz, in *Solid State Physics*, edited by H. Ehrenreich, F. Seitz, and D. Turnbull (Academic Press, New York, 1976), Vol. 31.
- ² N.K. Allen, P.J. Durham, B.L. Gyorffy, and R.G. Jordan, *J. Phys. F* **13**, 223 (1983).
- ³ H. Winter, P.J. Durham, and G.M. Stocks, *J. Phys. F* **14**, 1047 (1984).
- ⁴ S. Hüfner, G.K. Wertheim, and J.H. Wernick, *Solid State Commun.* **17**, 1585 (1975).
- ⁵ N. Mårtensson, R. Nyholm, H. Caleén, J. Hedman, and B. Johansson, *Phys. Rev. B* **24**, 1725 (1981).
- ⁶ P. Weightman, P.T. Andrews, G.M. Stocks, and H. Winter, *J. Phys. C* **16**, L81 (1983).
- ⁷ R.S. Rao, A. Bansil, H. Asonen, and M. Pessa, *Phys. Rev. B* **29**, 1713 (1984).
- ⁸ P. Weightman, M. Davies, and P.T. Andrews, *Phys. Rev. B* **30**, 5586 (1984).
- ⁹ M. Davies and P. Weightman, *J. Phys. C* **17**, L1015 (1984).
- ¹⁰ D. van der Marel, J.A. Jullianus, and G.A. Sawatzky, *Phys. Rev. B* **32**, 6331 (1985).
- ¹¹ H. Wright, P. Weightman, P.T. Andrews, W. Folkerts, C.F.J. Flipse, G.A. Sawatzky, D. Norman, and H. Padmore, *Phys. Rev. B* **35**, 519 (1987).
- ¹² P. Weightman, H. Wright, S.D. Waddington, D. van der Marel, G.A. Sawatzky, G.P. Diakun, and D. Norman, *Phys. Rev. B* **36**, 9098 (1987).
- ¹³ P.J. Braspenning, R. Zeller, A. Lodder, and P.H. Dederichs, *Phys. Rev. B* **29**, 703 (1984).
- ¹⁴ H. Winter, P.J. Durham, W.M. Temmerman, and G.M. Stocks, *Phys. Rev. B* **33**, 2370 (1986).
- ¹⁵ N. Stefanou, R. Zeller, and P.H. Dederichs, *Solid State Commun.* **62**, 735 (1987).
- ¹⁶ J. Kudrnovský and V. Drchal, *Solid State Commun.* **70**, 577 (1989).
- ¹⁷ J. Kudrnovský and V. Drchal, *Phys. Rev. B* **41**, 7515 (1990).
- ¹⁸ B. Ginatempo, G.Y. Guo, W.M. Temmerman, J.B. Staunton, and P.J. Durham, *Phys. Rev. B* **42**, 2761 (1990).
- ¹⁹ Z.W. Lu, S.-H. Wei, and A. Zunger, *Phys. Rev. B* **44**, 3387 (1991); **45**, 10314 (1992).
- ²⁰ S.K. Bose, J. Kudrnovský, O. Jepsen, and O.K. Andersen, *Phys. Rev. B* **45**, 8272 (1992).
- ²¹ J.J. Yeh and I. Lindau, *At. Data Nucl. Data Tables* **32**, 1 (1979).
- ²² I. Abbati, L. Braicovich, G. Rossi, I. Lindau, U. del Pennino, and S. Nannarone, *Phys. Rev. Lett.* **50**, 1799 (1983); G. Rossi, I. Lindau, L. Braicovich, and I. Abbati, *Phys. Rev. B* **28**, 3031 (1983).
- ²³ T.-U. Nahm, M. Han, S.-J. Oh, J.-H. Park, J.W. Allen, and S.-M. Chung, *Phys. Rev. Lett.* **70**, 3663 (1993).
- ²⁴ *Binary Alloy Phase Diagrams*, edited by T.B. Massalski (American Society for Metals, Metals Park, OH, 1986).
- ²⁵ G. Betz, *Surf. Sci.* **92**, 283 (1980).
- ²⁶ P.J. Feibelman and D.E. Eastman, *Phys. Rev. B* **10**, 4932 (1974).
- ²⁷ W. Speier, J.C. Fuggle, P. Durham, R. Zeller, R.J. Blake, and P. Sterne, *J. Phys. C* **21**, 2621 (1988).
- ²⁸ W.A. Harrison, *Electronic Structure and the Properties of Solids* (Freeman, San Francisco, 1980).
- ²⁹ N.E. Christensen, *J. Phys. F* **8**, L51 (1978).
- ³⁰ U. König, P. Marksteiner, J. Redinger, and P. Weinberger, and H. Ebert, *Z. Phys. B* **65**, 139 (1986).
- ³¹ P. Weightman, R.J. Cole, C. Verdozzi, and P.J. Durham, *Phys. Rev. Lett.* **72**, 793 (1994).
- ³² A.H. MacDonald, J.M. Daams, S.H. Vosko, and D.D. Koelling, *Phys. Rev. B* **25**, 713 (1982).
- ³³ P. Weinberger, A.M. Boring, R.C. Albers, and W.M. Temmerman, *Phys. Rev. B* **38**, 5357 (1988); G.K. Wertheim, L.F. Mattheiss, and D.N.E. Buchanan, *ibid.* **38**, 5988 (1988).
- ³⁴ L. Hedin and S. Lundquist, in *Solid State Physics*, edited by H. Ehrenreich, F. Seitz, and D. Turnbull (Academic Press, New York, 1969), Vol. 23.
- ³⁵ The Pd spectral weight including the self-energy of the model Hamiltonian with on-site Coulomb correlations was calculated in M. Cini and C. Verdozzi, *J. Phys. Condens. Matter* **1**, 7457 (1989), but a detailed form of $\Sigma(E)$ was not given.
- ³⁶ G. Tréglia, F. Ducastelle, and D. Spanjaard, *J. Phys. (Paris)* **43**, 341 (1982).
- ³⁷ E. Tamura, W. Piepke, and R. Feder, *J. Phys. Condens. Matter* **1**, 6469 (1989).
- ³⁸ M. Vos, G.A. Sawatzky, M. Davies, P. Weightman, and P.T. Andrews, *Solid State Commun.* **52**, 159 (1984).
- ³⁹ M. Vos, D.v.d. Marel, and G.A. Sawatzky, *Phys. Rev. B* **29**, 3073 (1984); M. Vos, D.v.d. Marel, G.A. Sawatzky, M. Davies, P. Weightman, and P.T. Andrews, *Phys. Rev. Lett.* **54**, 1334 (1985).
- ⁴⁰ G. Hörmandinger, P. Weinberger, and J. Redinger, *Phys. Rev. B* **40**, 7989 (1989).
- ⁴¹ D.R. Jennison, *Phys. Rev. Lett.* **40**, 807 (1978).

⁴² U. Scheuer and B. Lengler, Phys. Rev. B **44**, 9883 (1991); we might mention that this result was published *after* the Auger analysis of Refs. 38 and 39.

⁴³ In our previous Reply to the Comment by P. Weightman *et al.* [Phys. Rev. Lett. **72**, 794 (1994)], we stated that “the Pd Auger spectra of Mg-Pd, Al-Pd, and Ag-Pd alloys are

inadequate examples for the present issue, since Pd PDOS in these alloys are quite narrow due to their split-band behavior.” But we now agree that the Auger spectrum of the Pd impurity in a Ag host is in fact very sensitive to the amount of Pd bonding states, and is pertinent to the present issue.